ACI MATERIALS JOURNAL TECHNICAL PAPER

Title no. 86-M25

Tensile Stress-Strain Properties of SIFCON


by Antoine E. Naaman and Joseph R. Homrich

Slurry-infiltrated fiber concrete (SIFCON) composites differ from conventional fiber reinforced concrete in at least two aspects: they contain a much larger volume fraction of fibers and they use a matrix consisting of very fine particles. As such, they could be made simultaneously to exhibit outstanding strength and ductility properties. This research deals with the tensile stress-strain properties of SIFCON and comprises an experimental and an analytical program. Parameters investigated include the matrix composition and the fiber type where length, aspect ratio, surface characteristics, and overall fiber geometry vary. It is shown that SIFCON composites can exhibit tensile strength up to 4 ksi (28 MPa) at peak strains ranging from 1 to 2 percent. A model is proposed to predict the ascending branch of the stress-strain curve of SIFCON from its compressive strength and its fiber-reinforcing parameters.

Keywords: ductility; **fiber reinforced concretes; metal fibers; slurries;** strength; stress-strain relationships; **tensile strength;** tension tests.

Slurry-infiltrated fiber concrete (SIFCON) is a type of fiber reinforced concrete in which formwork molds are filled to capacity with fibers and the resulting fiber network is infiltrated by a cement-based slurry. Infiltration usually is accomplished by gravity flow aided by light vibration, or by pressure grouting.

SIFCON composites differ from conventional fiber reinforced concrete (FRC) in at least two aspects: they contain a much larger volume fraction of fibers and they use a matrix consisting of very fine particles. As such, they could be made simultaneously to exhibit outstanding strength and ductility properties.

From the behavioral viewpoint, the fibers in SIFCON are subjected to frictional and mechanical interlock in addition to the usual bond with the matrix. In SIFCON, the matrix plays the role not only of transferring forces between fibers by shear (as in FRC), but also of acting as a bearing to keep the fibers interlocked.

To date, most studies of SIFCON have dealt with its compressive[1-7] and flexural[8,9] behavior. Limited information exists on its tensile and shear properties.[10,11] However, available results indicate that SIFCON's performance may be as impressive in tension as it is in compression and flexure.

The main objective of this study is to provide a better understanding of the stress-strain response of high-strength slurry-infiltrated fiber concrete in direct uniaxial tension. Additional parameters investigated include the fiber type where length, aspect ratio, surface characteristics, and overall fiber geometry vary; and matrix composition.

RESEARCH SIGNIFICANCE

This research should provide a better understanding of the mechanisms of fiber reinforcement in SIFCON and the variables that control its tensile strength, stress-strain response, toughness, and fracture properties. The stress-strain curves and results presented can be considered among the first published in the technical literature. This paper summarizes some of the experimental observations and offers a simple analytical model to predict the stress-strain response of SIFCON in tension.

EXPERIMENTAL PROGRAM

The experimental program consists of uniaxial tensile tests on 18 in. (457 mm) dogbone-shaped prism specimens with a 3 x 1.5 in. (76 x 38 mm) testing area (Fig. 1). Two fiber types, hooked and deformed (Table 1 and Fig. 2), and, for each fiber type, two slurry mixes (Mixes 1 and 4 of Table 2) were investigated. Four specimens were placed for each variable.

Note that the slurry mixes are the same as those described in Reference 7 and were not renumbered here for consistency and continuity. Data from the tests were collected, processed, and analyzed to produce stress-strain relationships and to allow rational comparisons between the various parameters under study.

ACI Materials Journal, V. 86, No. 3, May-June 1989.
Received Dec. 28, 1987, and reviewed under Institute publication policies.

Antoine E. Naaman, FACI, is a professor of civil engineering at the University of Michigan, Ann Arbor. He is a member of Joint ACI-ASCE Committees 343, Concrete Bridge Design; and 423, Prestressed Concrete; and of ACI Committees 363, High Strength Concrete; 446, Fracture Mechanics; 544, Fiber Reinforced Concrete; and 549, Ferrocement. His research interests include high-strength high-performance cementitious composites and partially prestressed concrete.

***Joseph R. Homrich** is a naval engineer at the Norfolk Naval Shipyard, Portsmouth, Virginia. He received an MSc in civil engineering from the University of Michigan and was the recipient of the ACI Harry Thomson Scholarship for 1985.*

Dogbone-shaped plexiglass molds were especially built for the tensile specimens. The procedures for fiber placement, slurry mixing, placing, and specimen curing were the same as those described in a previous study on compression specimens.[7] The fibers were hand distributed into the molds and oriented as much as practicable in a direction parallel to the loading axis of the test specimens. The molds were placed on a vibrating table and subjected to light vibration during fiber placement. Alignment was more effective in the narrow testing region of the molds.

After 1 week of immersed curing in water, followed by about 2 months of air curing in the laboratory environment at approximately 70 F, all specimens were tested in uniaxial tension. Testing at a later age was desirable to better reflect the late strength development of the matrix that contained fly ash.

TESTING

The testing system consisted of a computer-controlled closed-loop servohydraulic universal testing machine, tensile friction grips, and a high-speed data acquisition system. The tensile friction grips and the fixture attachment to the specimen are shown in Fig. 3. The grips consisted of self-clamping steel plates and a universal joint connection to the loading machine, which allowed freedom of rotation along coordinate axes and eliminated the possibility of inducing end moments in the specimens (Fig. 3). During the tests, load and deformation data were recorded and stored by the data acquisition system and later processed for analysis.

Two linear voltage differential transducers (LVDTs) were placed on opposite sides of the specimen at a predetermined gage spacing of 6 in. (150 mm). The signal from each LVDT was conditioned and recorded by an analog-to-digital converter as specimen deformation data. The load signal was taken directly from the testing machine control computer.

The tension tests were run using stroke control at two different loading rates. A rate of 0.001 in./sec (166 microstrains/sec) was employed during the initial ascending branch of the stress-strain curve up to the point of maximum stress. The stroke rate was reduced as failure proceeded in an attempt to record a significant part of the descending branch of the stress-strain curve and minimize the effect of machine energy release. The stroke rate often was reduced to 10^{-6} in./sec (0.166 microstrains/sec) before complete specimen separation occurred.

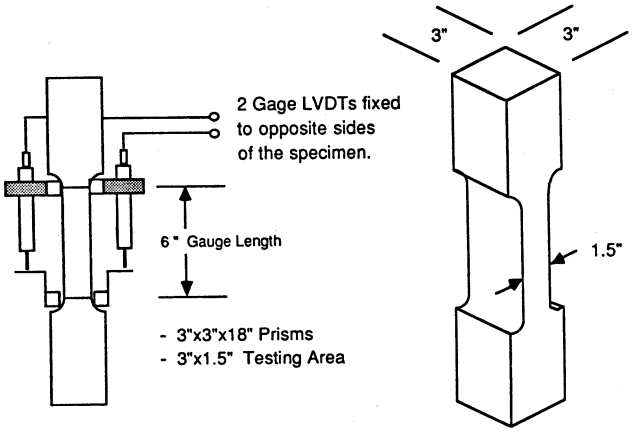

Fig. 1—Tension dogbone specimens

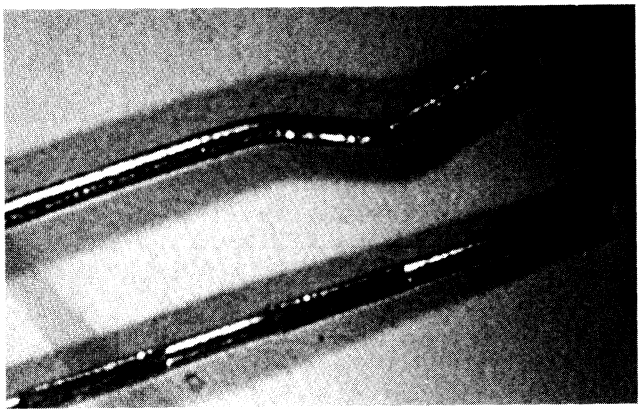

Fig. 2—Fibers used in this investigation

Table 1 — Fiber properties

Fiber type	Length, mm	Diameter, mm	Aspect ratio *l/d*	Yield stress, ksi (MPa)	Volume fraction,* percent
Hooked	30	0.5	60	170 (1190)	11 to 13
Deformed	30	0.5	60	N.A.	12 to 14

*Assuming fibers are placed primarily aligned with the loading direction.

RESULTS, DISCUSSION, AND ANALYSIS

Stress-strain response

Fig. 4 shows a typical tensile load-elongation response up to complete separation as recorded from the data. For the purpose of discussion, the curve may be divided into two parts: an ascending branch up to the peak load, and a descending branch from the peak load to complete separation. The elongation up to the peak load can be translated into tensile strain (where strain equals elongation divided by gage length). The elongation beyond the peak load represents primarily the opening of a critical crack and cannot be directly used as a strain.

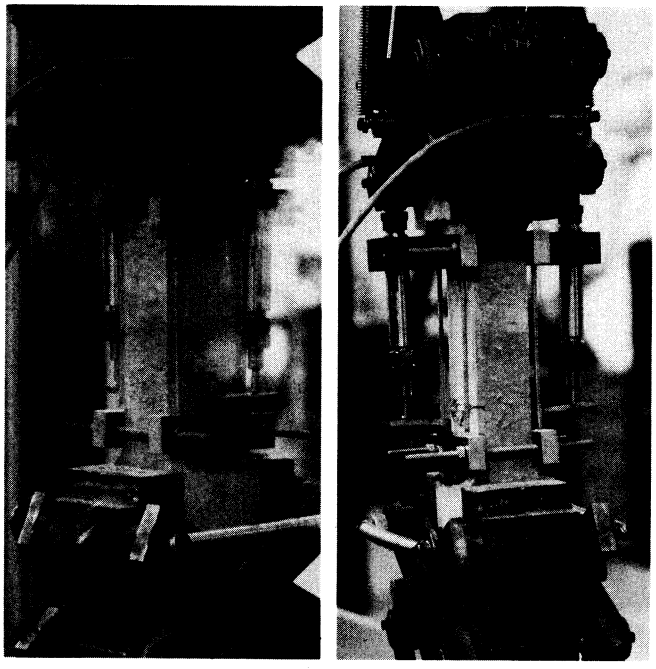

Fig. 3—Friction grips and specimens under test

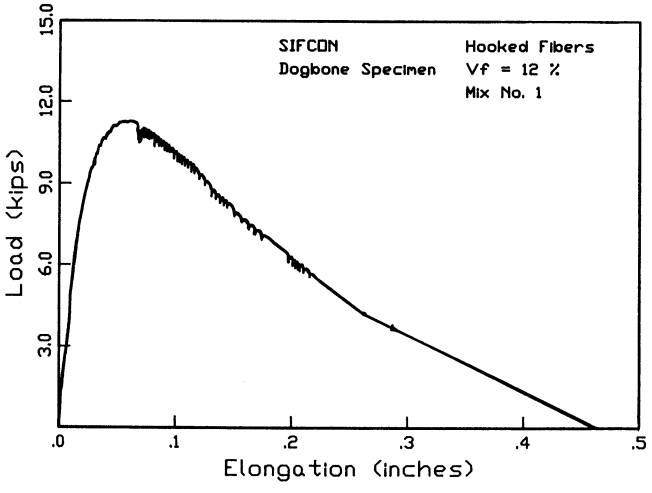

Fig. 4—Typical load-elongation curve of SIFCON in tension

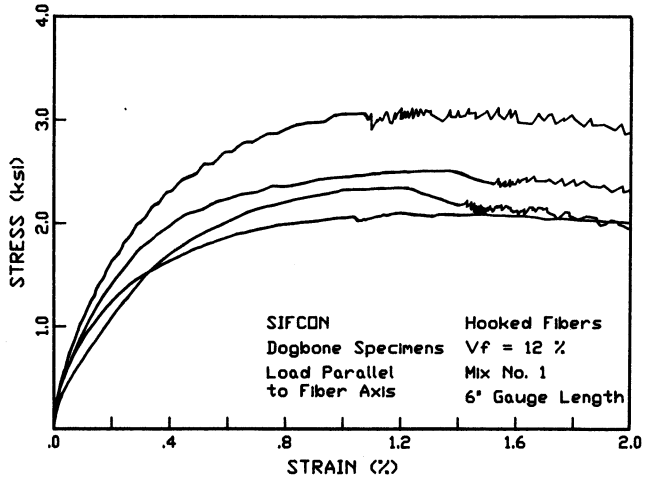

Fig. 5—Typical stress-strain response with hooked fibers

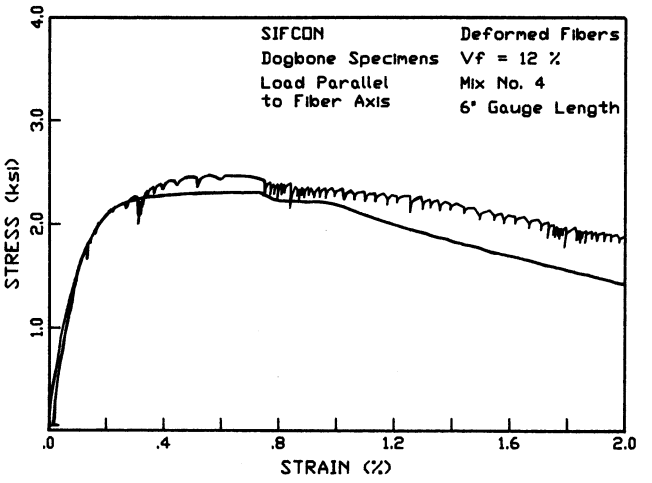

Fig. 6—Typical stress-strain response with deformed fibers

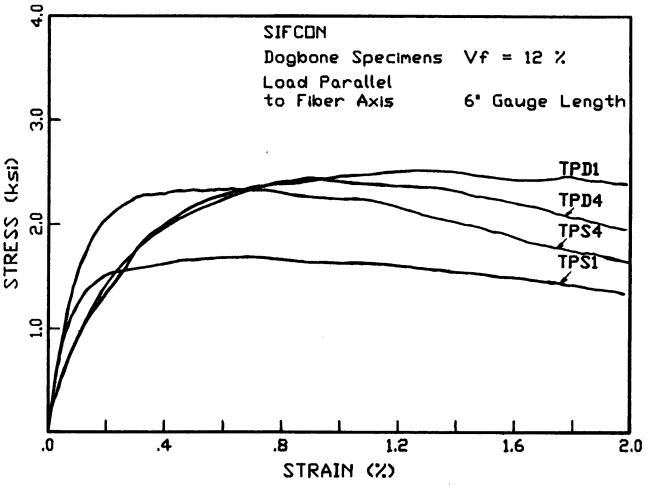

Fig. 7—Typical comparison between test series

Fig. 5 and 6 show typical graphical results of the tensile tests where the strains are plotted up to an equivalent value of 2 percent. Fig. 7 illustrates a comparison between the stress-strain response of the four series of tests with specimens containing about 12 percent fibers by volume. The nomenclature used in Fig. 7 is as follows: "T" stands for tension, "P" for parallel, "D" for hooked fibers, "S" for deformed fibers, "1" for Slurry Mix 1, and "4" for Slurry Mix 4 (Tables 1 and 2). Two immediate observations can be made from these figures, namely, the ascending branch of the stress-strain curve is highly nonlinear, and the strains to the peak load and to failure are very large in comparison to plain concrete. Additional observations are reported in the two following sections.

Ascending branch—As testing begins, the curve is linear over a small portion, then gradually becomes nonlinear as the maximum load is approached. The nonlinearity of the curve is caused primarily by multiple cracking in the testing zone. These cracks usually are small but clearly visible during testing and tend to be evenly distributed along the testing zone; however, they are not through cracks as in reinforced concrete and ferrocement. It should be noted that the end of the

Table 2 — Slurry mix proportions

Mix number*	Mix constituents	Relative weight	w/c†	f'_c range, ksi (MPa)
1	Type 1 cement	1.000		
	Fly ash	0.200	0.35	8 to 17
	Water	0.360		(56 to 120)
	Superplasticizer	0.030		
4	Type I cement	1.000		
	Fly ash	0.250	0.26	10 to 20
	Water	0.325		(70 to 140)
	Superplasticizer	0.040		

*Mix number 2 and 3 are described in Reference 7 for the compression tests but were not used for the tensile tests.
†Water-cementitious ratio equals ratio of water over combined cement plus fly ash.

linear portion of the curve does not necessarily represent the onset of cracking in the matrix but only the end of the composite elastic response. Indeed, many shrinkage cracks were observed on the surface of the specimens prior to testing.

The ascending branch region of the load-elongation response up to the peak stress (Fig. 4) can be translated into a stress-strain response of the composite. The upper end of this region is marked by the extension and opening of one of the many small tensile cracks (or crack clusters) in the testing zone. A peak point could be determined from each curve, but often a flat plateau could better describe the behavior near the peak. This is why Fig. 5 through 7 all have a maximum strain scale of 2 percent.

Descending branch—After the peak stress is attained, the failure proceeds as a single crack opening with fibers debonding on either side of the crack area. The opening of one large failure crack is accompanied by the release of strain energy in the testing system and the closing of microcracks in the testing zone. Typical cracking and failure modes are shown in Fig. 8 and 9. As the failure crack opens, recoverable stress-strain response is lost and the observed curve becomes instead a representation of load versus crack-opening response.

This response cannot be considered very useful since the failure crack is never truly planar nor perpendicular to the testing direction. Thus, an investigation of the stress-displacement (or stress-crack opening) response of a planar crack was undertaken, but the results are left for a future publication.

Average properties

Table 3 lists the average results of the tensile tests of SIFCON specimens for the four series investigated. The table lists important parameters including the elastic modulus up to 45 percent of peak stress, the composite strength, and the toughness index in comparison with normal strength concrete in tension. Since only a narrow spectrum of variables were involved in this study, comparisons are difficult to make. It can be noted that the combinations of two fibers and two matrices examined in this study resulted in composites with very similar stress-strain behavior. This is predictable since the matrices had similar strength ranges and the fibers had the same reinforcing index ($V_f l/d$) (see Tables 1 and 2).

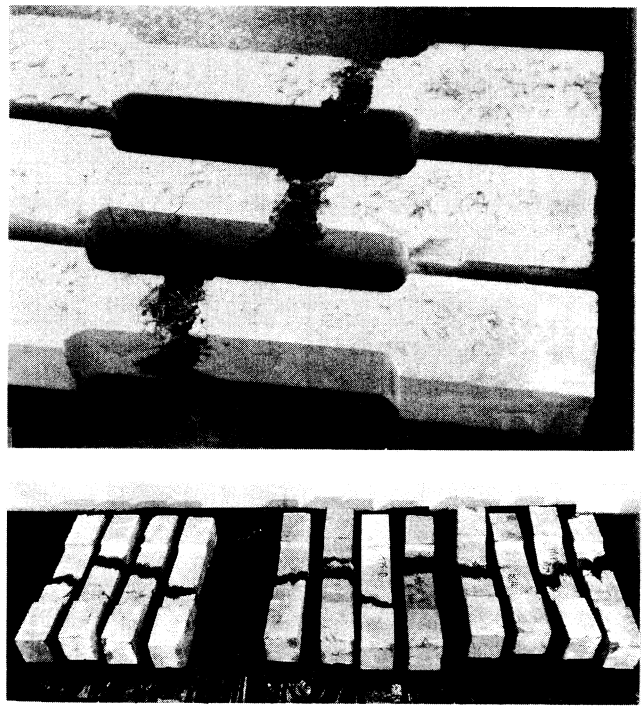

Fig. 8—Example of cracking and failure in tension

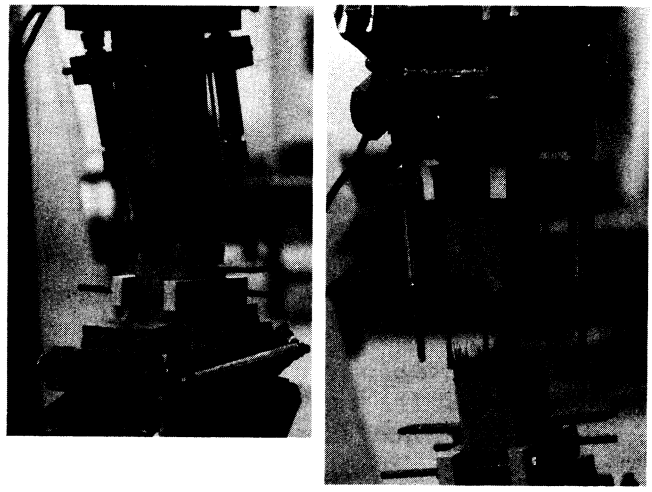

Fig. 9—Typical failure cracks

The performance of SIFCON in tension is quite impressive. The highest strength obtained in this part of the study was 3000 psi (21 MPa), an order of magnitude greater than would be expected of unreinforced normal concrete. Higher strength values [above 4000 psi (28 MPa)] were obtained from the tensile stress-displacement tests. The strains obtained at maximum stress (up to 1 percent with some recoverable elastic strain) are about two orders of magnitude greater than those of the unreinforced matrix. If the energy-absorption capacity of a material is defined as the area under the stress-strain curve, then the energy-absorption capacity of SIFCON is up to three orders of magnitude greater than that of the unreinforced matrix.

Table 3 presents this information in the form of a toughness index. The toughness index is defined in this paper as the area under the stress-strain curve of SIFCON up to 2 percent strain divided by the area under

Table 3 — Average tension test results

Series identification	Fiber volume, percent	Elastic modulus,* 10^3 ksi (MPa)	Maximum stress, ksi (MPa)	Strain at maximum stress, percent	Stress at 2 percent equivalent strain, ksi (MPa)	Toughness index†
TPD1D	11.7	0.665 (4.585)	2.26 (15.58)	1.29	2.24 (15.44)	770
TPS1D	12.6	1.480 (10.204)	1.58 (10.89)	0.61	1.19 (8.20)	570
TPD4D	12.1	0.665 (4.585)	2.28 (15.72)	1.21	1.98 (13.65)	770
TPS4D	13.8	2.010 (13.858)	2.34 (16.13)	0.68	1.68 (11.58)	800

*Secant modulus measured from origin to 45 percent of peak stress.
†Toughness index measured as area under stress-strain/load-deflection curve of SIFCON up to 2 percent strain divided by area under stress-strain curve of normal strength (5000 psi [34 MPa] compressive strength) concrete up to peak stress.

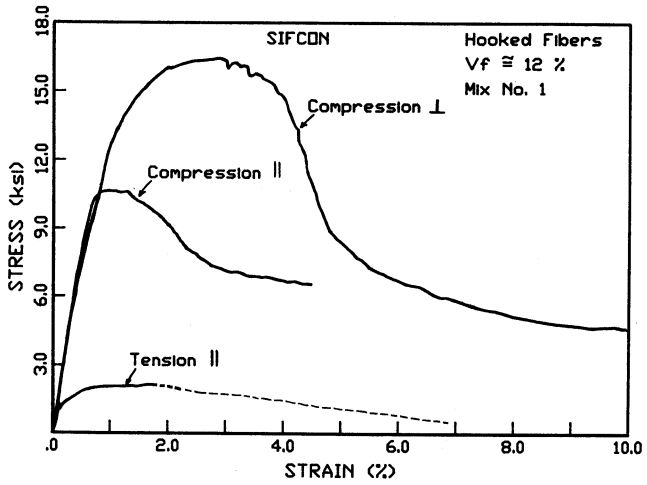

Fig. 10—Comparison between compression and tensile stress-strain curves—hooked fibers

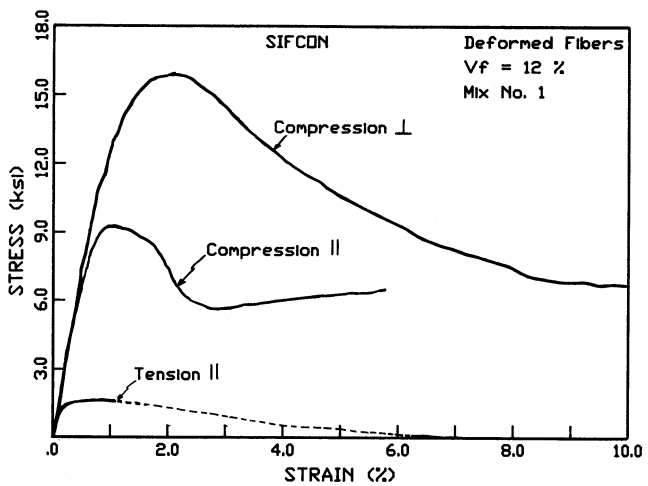

Fig. 11—Comparison between compression and tensile stress-strain curves—deformed fibers

the stress-strain curve of normal-strength concrete up to peak tensile stress. The toughness index of the series investigated in this study ranges from approximately 570 to 800.

Effect of fiber type and elastic modulus

Failure of SIFCON in tension takes place mostly through fiber pullout, fiber-matrix debonding, and loss of fiber-to-fiber interlock. No fiber failure was observed in this study. However, the length, strength, and geometry of the fibers used in the composite should have a significant influence on the composite's stress-strain behavior.

The similarity in reinforcing effects of the fibers and matrices examined in this study was pointed out earlier. Although the variability in strength results within series was normal, unexpectedly high variability was observed in the measurements of the elastic modulus of the composite. Moreover, the observed modulus of test specimens made with deformed fibers was substantially higher than that of specimens made with hooked fibers (Table 3). The reason for this behavior may need additional investigation; however, it is pointed out that the presence and extent of shrinkage cracks largely contributes to variations in the initial slope of the ascending portion of the stress-strain curve and corresponding modulus values obtained.

Two other factors may have contributed to the difference observed between the two fibers. First, the smooth surface of the hooked fibers (Fig. 2) may not restrain internal shrinkage cracking as well as the textured surface of the deformed fibers. This may lead to greater internal cracking and a material with lower stiffness. Second, because of their surface texture, deformed fibers may have, at small strains, a better matrix-to-fiber bond than the hooked fibers, thus resulting in a stiffer composite.

Comparison between tensile and compressive response

Fig. 10 and 11 show typical comparisons of the stress-strain response of SIFCON composites in tension and compression. Two curves are plotted for the compression tests, one corresponding to the case where the fibers are primarily normal to the loading axis and the other where the fibers are primarily parallel to the loading axis. The case of random fiber orientation should likely fall in between.

Like SIFCON in compression, specimens made with hooked and deformed fibers had very similar stress-

strain responses. The ultimate strengths obtained with the two types of fibers were close, as was the overall shape of their stress-strain curves. This may imply that many of the variables responsible for SIFCON's stress-strain behavior in compression also are responsible for its stress-strain behavior in tension and that a fiber's performance in compression will be indicative of its performance in tension. The curves of Fig. 10 and 11 suggest that the tensile strength of SIFCON ranges from about 15 to 25 percent of its compressive strength depending on the orientation of the fiber axis to the axis of loading.

Composite strength

Table 2 lists the range of composite strengths attained in this study. Since the two matrices studied in the tests were similar in design and composition, it is not surprising that similar strengths were obtained by all specimens. Thus, without additional testing, no conclusion may be drawn on how matrix strength influences the behavior of the composite. However, since the main function of the matrix in SIFCON composites in tension is to restrain fiber slip through bond and compressive clamping action, it seems likely that the tensile strength of the composite will increase with an increase in the compressive strength of the cementitious matrix.

Stress-strain curve nonlinearity

The nonlinearity observed in most stress-strain curves at small fractions of ultimate loads is apparent in Fig. 5 through 7. This nonlinear shape is due to the immediate opening of cracks and possible debonding of fibers during testing. Since the matrices involved are very strong, it is unlikely that load-induced cracking is responsible for the initial nonlinearity of the curve. The observed nonlinearity likely is due to the presence of cracks already in the matrix before testing. Such cracks probably are induced by drying-shrinkage cracking as explained previously.

ANALYTICAL MODELING

In principle, constitutive models for fiber reinforced composites can be derived from the knowledge of the properties of the components' materials and their interfaces. Such models should be sought for SIFCON as well as for conventional fiber reinforced cements and concretes. While a fundamental approach is desirable and may be attained through extensive research, it also may lead to a solution that is too complex to be attractive in practice.

As SIFCON is a relatively new material and as research is continuing on the fundamental modeling of its behavior, a simple semirational model is offered here to give an estimate of its stress-strain response in tension in terms of the fiber reinforcing parameters.

The proposed model requires the knowledge of the compression strength of SIFCON as obtained from a standard cylinder test; such information is much easier to obtain than any equivalent tensile properties.

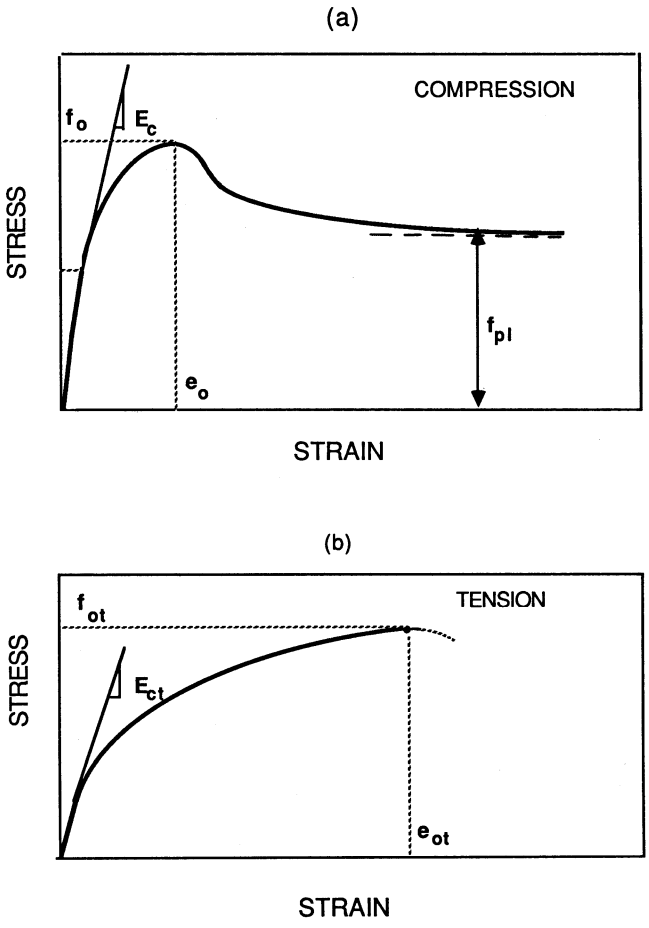

Fig. 12—Typical stress-strain curve of SIFCON: (a) in compression and (b) in tension

Fig. 12(a) shows a typical stress-strain curve of SIFCON in compression, and Fig. 12(b) shows the typical ascending branch of its tensile stress-strain curve. After a preliminary investigation in which several analytical prediction equations were tried to model the tensile response, the following equation is proposed

$$f = f_{ot}[1 - (1 - \epsilon/\epsilon_{ot})^D] \quad (1)$$

where f and ϵ are the tensile stress and corresponding strain in general, f_{ot} is the tensile strength of the composite, ϵ_{ot} is the strain at maximum tensile stress, and the parameter D is given by

$$D = E_c \epsilon_{ot}/f_{ot} \quad (2)$$

in which E_c is the initial tangent modulus of the composite.

To determine the tensile strain at maximum stress, the following prediction equation was found acceptable

$$\epsilon_{ot} = \epsilon_{su} + KV_f l/d \quad (3)$$

where ϵ_{su} is the ultimate tensile strain of the unreinforced slurry, V_f is the volume fraction of fibers, l is their length, and d is their diameter. By averaging the test data of this investigation, the following values of ϵ_{su} and K were obtained

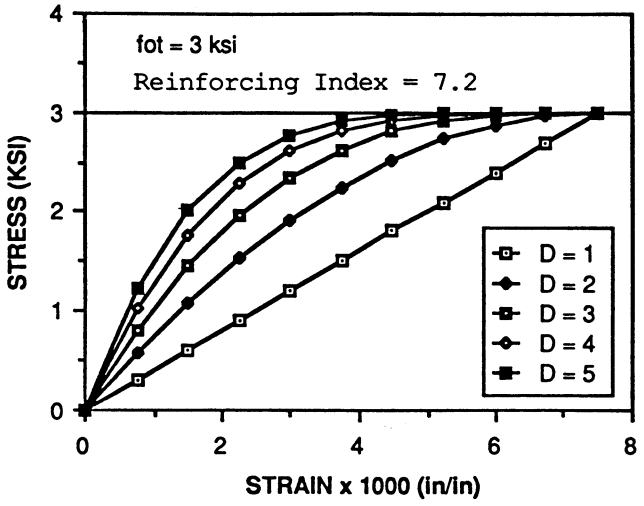

Fig. 13—Analytically generated stress-strain response in tension

$\epsilon_{su} = 0.0005$

$K = 0.00097$ for deformed fibers and 0.00174 for hooked fibers

These results assume that the fibers are aligned primarily parallel to the loading direction. It should be noted that an equation similar to Eq. (1) was used in Reference 12 to predict the ascending branch of the stress-strain curve of plain and confined concrete in compression. Since it depends on only three parameters, its use for the tensile response of SIFCON was found more convenient than the relationship used earlier in Reference 13 for fiber reinforced mortar.

To predict the ultimate tensile strength of a SIFCON material, a test on its compressive strength is needed. Indeed, a correlation was found in this study between the tensile strength and the compressive post-peak plateau stress in compression, assuming the fibers are primarily parallel to the loading direction. This correlation can be explained by pointing out that the compressive post-peak stress is a response to shear mode failure and that there is, in general, a strong correlation between shear strength and tensile strength. This yielded the following approximation for the tensile strength of SIFCON

$$f_{ot} = \alpha f_{pl} \qquad < V_f f_{fu} \tag{4}$$

where f_{pl} is the post-peak plateau stress in compression [Fig. 11(a)], α is a coefficient, and f_{pu} is the tensile strength of the fibers. Eq. (4) holds only when f_{ot} is larger than the cracking strength of the unreinforced slurry matrix. For the parameters used in this study, α was found to equal approximately ⅓. The value of f_{pl} can be estimated from

$$f_{pl} = V_f l/d\,(200 + 8\sqrt{f_o}) \text{ in psi}$$
$$f_{pl} = V_f l/d\,(1.4 + 0.66\sqrt{f_o}) \text{ in MPa} \tag{5}$$

where f_o is the compressive strength from standard cylinder tests.

The modulus of elasticity of SIFCON, as used in Eq. (2), could be measured from standard tests in compression and/or tension on wet specimens. Theoretically, compression or tension tests should lead to the same value of initial modulus. However, due to the influence of shrinkage cracking, elastic modulus values obtained from tension tests may differ significantly from those obtained from compression tests.

An attempt to use the law of mixtures to predict the elastic modulus led to values two to three times larger than those observed in the experiments. The law of mixtures was thus modified to reflect the observed data. It led to the following prediction equation for the elastic modulus of SIFCON in tension

$$E_{ct} = k\,V_f E_f + V_m E_m = kV_f E_f + (1 - V_f)E_m \tag{6}$$

in which k is a factor derived from the data and the subscripts f, m, and c refer to the fiber, matrix, and composite, respectively. For the range of variables used in this investigation and ongoing additional tests, a value of k about ⅓₀ for fibers aligned primarily parallel to the loading axis and a value of E_m of about 1000 ksi (7000 MPa) can be used as a first approximation in Eq. (6).

In summary, given the compressive strength f_o [Fig. 12(a)] of SIFCON as obtained from a cylinder test, and given the fiber reinforcing parameters, the compressive plateau stress f_{pl} [Fig. 12(a)] may be estimated from Eq. 5, and the parameters D, E_{ct}, ϵ_{ot}, and f_{ot} may be estimated from Eq. (2) through (4), respectively. Then the ascending branch of the tensile stress-strain curve of SIFCON can be predicted from Eq. (1).

An example of analytically generated curves illustrating the influence of the parameter D [Eq. (2)] is shown in Fig. 13.

CONCLUSIONS

The following conclusions may be drawn from the tension tests of SIFCON specimens containing about 12 percent steel fibers by volume:

1. Tensile strength—In this study, the use of Slurry Mixes 1 and 4 with hooked and deformed fibers led to average tensile strengths of 1.6 to 2.3 ksi (11 to 16 MPa) with a maximum observed strength of 3.0 ksi (21 MPa). Tests on notched specimens led to strengths as high as 4 ksi (28 MPa).

2. Tensile ductility—SIFCON specimens are able to sustain tensile stresses of about 2 ksi (14 MPa) reliably at tensile strains ranging from 1 to 2 percent.

3. Internal drying-shrinkage cracking of SIFCON composites may lead to a poorer material stress-strain performance, resulting in a highly nonlinear ascending portion of the stress-strain response.

4. The early nonlinearity of SIFCON's stress-strain response is less pronounced with deformed fibers than with hooked fibers. This is probably the result, at small tensile strains, of better local fiber-to-matrix bonding and fiber-to-fiber interlock with deformed fibers.

5. SIFCON composites exhibit multiple cracking at low and intermediate load levels. Final failure occurs through the opening of a single large tensile crack.

6. Compared to plain slurry, the toughness index of SIFCON in tension evaluated at 2 percent strain can reach 1000.

The cracking of SIFCON prior to loading appears attributable to drying shrinkage since cracking appears in specimens only during air curing. The extensiveness and severity of the cracking observed in the test specimens suggests that this phenomenon has the potential to be a real durability problem. Further research into the problem of drying-shrinkage cracking of low water-cementitious ratio composites is desirable.

ACKNOWLEDGMENT

This study was supported by grant No. F29601-85-K-0069 from the Air Force Weapons Laboratory, Civil Engineering Research Division, to the University of Michigan, with Captain Susan Cheney as Air Force project task officer. Their support and cooperation are gratefully appreciated. Any opinions, findings, and conclusions expressed in this paper are those of the writers and do not necessarily reflect the views of the sponsor.

REFERENCES

1. Lankard, David R., and Lease, Daniel H., "Highly Reinforced Precast Monolithic Refractories," *American Ceramic Society Bulletin,* V. 61, No. 7, July 1982, pp. 728-732.

2. Lankard, David R., and Newell, Jeffrey K., "Preparation of Highly Reinforced Steel Fiber Reinforced Concrete Composites," *Fiber Reinforced Concrete—International Symposium,* SP-81, American Concrete Institute, Detroit, 1984, pp. 277-306.

3. Lankard, D. R., "Slurry Infiltrated Fiber Concrete (SIFCON): Properties and Applications," *Very High Strength Cement Based Composites,* V. 42, Materials Research Society, Pittsburgh, 1985, pp. 227-286.

4. "Summary Report on Preparation and Properties of Slurry Infiltrated Fiber Concrete (SIFCON) prepared with Four Bekaert Steel Fibers," Lankard Materials Laboratory, Inc., Columbus, Feb. 1985.

5. Schneider, B.; Mondragon, R.; and Kirst, J., "Task Report NMERI, TAB-69 (8.36-01)," New Mexico Engineering Research Institute, June 1984, 83 pp.

6. Mondragon, R., "Development of Material Properties for Slurry Infiltrated Fiber Concrete (SIFCON)—Compressive Strength," *Technical Report* No. NMERI WA8-18 (8.03), New Mexico Engineering Research Institute, Dec. 1985, 394 pp.

7. Homrich, J. R., and Naaman, A., "Stress-Strain Properties of SIFCON in Compression," *Fiber Reinforced Concrete—Properties and Applications,* SP-105, American Concrete Institute, Detroit, 1987, pp. 283-304.

8. Balaguru, P., and Kendzulak, John, "Flexural Behavior of Slurry Infiltrated Fiber Concrete (SIFCON) Made Using Condensed Silica Fume," *Fly Ash, Silica Fume, Slag, and Natural Pozzolans in Concrete,* SP-91, American Concrete Institute, Detroit, 1986, pp. 1215-1229.

9. Baggott, R., and Sarandily, A., "Very High Strength Steel Fiber Reinforced Autoclave Mortars," *Proceedings,* 3rd RILEM International Symposium on Developments in Fiber Reinforced Cement and Concrete, Sheffield, V. 1, Sec. 3, Paper 3.5, July 1986.

10. Balaguru, P., and Kendzulak, J., "Mechanical Properties of Slurry Infiltrated Fiber Concrete (SIFCON)," Fiber Reinforced Concrete—Properties and Applications, SP-105, American Concrete Institute, Detroit, 1987, pp. 247-268.

11. Naaman, A.E., "Advances in High Performance Fiber Reinforced Cement Composites," *Proceedings* IABSE Symposium on Concrete Structures for the Future (Paris, 1987), International Association for Bridge and Structural Engineering, Zürich, pp. 371-376.

12. Shah, Surendra P.; Fafitis, Apostolos; and Arnold, Richard, "Cyclic Loading of Spirally Reinforced Concrete," *Journal of Structural Engineering,* ASCE, V. 109, No. 7, July 1983, pp. 1695-1710.

13. Fanella, David A., and Naaman, Antoine E., "Stress-Strain Properties of Fiber Reinforced Mortar in Compression," ACI JOURNAL, *Proceedings* V. 82, No. 4, July-Aug. 1983, pp. 475-483.